

# Exploration of biguanido–oxovanadium complexes as potent and selective inhibitors of protein tyrosine phosphatases

Liping Lu · Xiaoli Gao · Miaoli Zhu ·  
Sulian Wang · Qiong Wu · Shu Xing ·  
Xueqi Fu · Zhiwei Liu · Maolin Guo

Received: 21 December 2011 / Accepted: 12 April 2012 / Published online: 1 May 2012  
© Springer Science+Business Media, LLC. 2012

**Abstract** The inhibitory effects of three biguanido–oxovanadium complexes ( $[\text{VO}(\text{L}^{1-3})_2] \cdot n\text{H}_2\text{O}$ :  $\text{HL}^1 =$  metformin,  $\text{HL}^2 =$  phenformin,  $\text{HL}^3 =$  moroxydine) against four protein tyrosine phosphatases (PTPs) and an alkaline phosphatase (ALP) were investigated. The complexes display strong inhibition against PTP1B and TCPTP ( $\text{IC}_{50}$ , 80–160 nM), a bit weaker inhibition against HePTP ( $\text{IC}_{50}$ , 190–410 nM) and SHP-1 ( $\text{IC}_{50}$ , 0.8–3.3  $\mu\text{M}$ ) and much weaker inhibition against ALP

( $\text{IC}_{50}$ , 17–35  $\mu\text{M}$ ). Complex **3** is about twofold less potent against PTP1B, TCPTP and HePTP than complexes **1** and **2**, while complex **2** inhibits SHP-1 more strongly (about three to fourfold) than the other two complexes. These results suggest that the structures of the ligands slightly influence the potency and selectivity against PTPs. The complexes inhibit PTP1B and ALP with a typical competitive type.

**Keywords** Biguanido–oxovanadium complexes · Protein tyrosine phosphatases · Competitive inhibition · Selective inhibition

S. Wang is a teacher of Xuanhua County NO.1 Middle School of Hebei Province, P. R. China.

L. Lu · X. Gao · M. Zhu (✉) · S. Wang  
Institute of Molecular Science, Key Laboratory of  
Chemical Biology and Molecular Engineering of the  
Education Ministry, Shanxi University, Taiyuan 030006,  
Shanxi, People's Republic of China  
e-mail: miaoli@sxu.edu.cn

X. Gao  
Department of Chemistry, Taiyuan Normal University,  
Taiyuan 030001, People's Republic of China

Q. Wu · S. Xing (✉) · X. Fu  
Edmond H. Fischer Signal Transduction Laboratory,  
College of Life Sciences, Jilin University, Changchun  
130023, People's Republic of China  
e-mail: xingshu@jlu.edu.cn

Z. Liu · M. Guo (✉)  
UMass Cranberry Health Research Center, Department of  
Chemistry and Biochemistry, University of Massachusetts  
Dartmouth, Dartmouth, MA 02747, USA  
e-mail: mguo@umassd.edu

## Introduction

Protein tyrosine phosphatases (PTPs) are key modulators in various signal transduction pathways (Alonso et al. 2004; Zhang and Zhang 2007). Dysregulation of PTP activities contributes to the pathogenesis of several human diseases, including diabetes, obesity, cancer and immune disorders (Andersen et al. 2004; Arena et al. 2005; Zhang 2001). The importance of PTPs in diverse pathogenesis has made them promising targets for drug discovery (Combs et al. 2005; Dewang et al. 2005). Among various members in the PTP superfamily, protein tyrosine phosphatase 1B (PTP1B), a key negative regulator of insulin signaling, has emerged as an attractive target for the treatment of type II diabetes. PTP1B directly inactivates the insulin receptor by dephosphorylating tyrosine residues in the

regulatory domain (Kenner et al. 1996; Saltiel and Kahn 2001), and its overexpression inhibits insulin signaling (Byon et al. 1998). PTP1B gene knockout and antisense studies in normal and diabetic mice have shown lower blood glucose levels and improved insulin responsiveness through enhanced insulin receptor signaling in peripheral tissues (Elchebly 1999; Klamman et al. 2000; Zinker et al. 2002). Therefore, PTP1B inhibitors have been pursued to develop novel anti-diabetic drugs (Ala et al. 2006; Maccari et al. 2007; Na et al. 2006; Shrestha et al. 2007; Sparks et al. 2007; Winter et al. 2005; Xie and Seto 2007). PTPs contain a highly conserved catalytic motif signature of (I/V)HCXAGXXR(S/T)G, therefore, it is challenging to develop selective inhibitors targeting a special PTP such as PTP1B although a few inhibitors with some selectivity toward certain PTPs have been reported (Iversen et al. 2000; Liljebris et al. 2002; Na et al. 2006; Xie and Seto 2007).

Numerous studies have demonstrated that vanadium compounds have insulin-enhancing effects and can improve the symptoms of diabetes in a variety of animal models (Crans et al. 2004; Rehder 2003; Shechter 2003). Organovanadium compounds have been shown to have superior insulin mimetic compared to sodium orthovanadate (Drake and Posner 1998; Posner et al. 1994; Reul et al. 1999; Willsky et al. 2001). Bis(ethylmalto)oxovanadium(IV) (BEOV) was tested on phase II clinical trials as an anti-diabetic drug (Thompson et al. 2009). The mechanism of action of vanadium's insulin-sensitizing effects has not been well understood but association with protein tyrosine phosphatase inhibition has been implicated. Some vanadium compounds have been shown to directly inhibit some PTPs including PTP1B (Huyer et al. 1997; Nxumalo et al. 1998; Peters et al. 2003; Posner et al. 1994). It is generally assumed that vanadate is an unspecific and potent phosphatase inhibitor since it shares a similar structure with phosphate. Recently, we have been exploring novel vanadium complexes as PTP1B inhibitors (Gao et al. 2009; Lu et al. 2010, 2011; Yuan et al. 2009, 2010). Interestingly, [VO(IV)(SAA)(bpy)] complex selectively inhibits PTP1B over the other two phosphatases Src homology phosphatase 1 (SHP-1) and T-cell protein tyrosine phosphatase (TCPTP), however oxovanadium glutamate complex inhibits the PTP1B, TCPTP, SHP-1 and HePTP with almost same potency.

Biguanide derivatives, such as metformin, are currently used worldwide for the treatment of type 2

diabetes mellitus. Preliminary animal investigations indicate that a bi-functional biguanido–oxovanadium complex  $\text{VO}(\text{L}^1)_2$  is comparable to BMOV in lowering blood glucose in STZ-diabetic rats (Woo et al. 1999). Here we have investigated the effects of biguanido–oxovanadium complexes on four PTPs and alkaline phosphatase (ALP). The results indicate that these complexes are potent inhibitors against PTPs with little selectivity towards PTP1B, TCPTP and HePTP (hematopoietic tyrosine phosphatase). However they are obviously less potent in inhibiting SHP-1 and ALP. These results imply that although vanadium complexes generally lack specificity in inhibiting PTPs, the ligands on vanadium can contribute to the selectivity against different PTPs.

## Experimental

### Materials and physical measurements

Calf intestinal ALP ( $1,000 \text{ U mL}^{-1}$ ) and its  $10\times$  buffer were products of Sigma Chemie GmbHV (Taufkirchen, Germany). GSH and *p*-nitrophenol phosphate (*p*-NPP) were purchased from Huamei Biotechnologies (Beijing, China) and Ceibo Technologies (Shanghai, China), respectively. Three N-substituted derivatives of biguanide, metformin ( $\text{HL}^1\cdot\text{HCl}$ ,  $N,N'$ -dimethylbiguanide hydrochloride), phenformin ( $\text{HL}^2\cdot\text{HCl}$ ,  $\beta$ -phenethylbiguanide hydrochloride), moroxydine ( $\text{HL}^3\cdot\text{HCl}$ , morpholinebiguanide hydrochloride) were presented by Wujin Medicine Raw Material Chemical Factory of China. Other chemicals and solvents were AR grade and were purchased commercially without further purification. Double distilled water was used to prepare buffer solutions.

IR spectra were recorded on a Shimadzu FT IR-8300 spectrometer in the range of  $4,000\text{--}400 \text{ cm}^{-1}$  as KBr pellets. Elemental analysis for C, H, and N was determined by microanalysis using a Perkin-Elmer 240B elemental analyzer. UV–Visible spectra were measured with a HP-8453 UV–Vis spectrophotometer. Fluorescence emission spectra were recorded on a Cary Eclipse spectrophotometer (Varian USA). Bioactivity assays of the compounds were carried out on a Bio-RAD model 550 microplate reader. The pH values were measured on a digital display pH meter (PHS-3TC, Shanghai Tianda Instrument Co. Ltd., of China).

## Preparation and characterization of biguanide complexes

The biguanido–oxovanadium complexes were synthesized following the literature (Woo et al. 1999) with slightly modification. Briefly,  $\text{VOSO}_4$  (5 mmol) in solution was added into an aqueous solution of N-substituted derivatives of biguanide hydrochloride (10 mmol) with a constant stirring. Adjusted pH to the range of 10–11 by NaOH, the solution was stirred for 2 h until precipitation was completed. Then the precipitates were collected by filtration, washed with water, ethanol, and diethyl ether, respectively, and dried overnight in a vacuum desiccator with  $\text{P}_2\text{O}_5$ . The products,  $[\text{VO}(\text{L}^1)_2] \cdot \text{H}_2\text{O}$  (**1**),  $[\text{VO}(\text{L}^2)_2] \cdot 2\text{H}_2\text{O}$  (**2**) and  $[\text{VO}(\text{L}^3)_2] \cdot \text{H}_2\text{O}$  (**3**), were characterized by elemental analysis, IR and UV–Vis spectroscopy (Table 1).

## Potentiometric titration

pH-potentiometric titrations in aqueous solutions were performed at  $298.0 \pm 0.2$  K. The ionic strength was adjusted to 0.1 M with  $\text{NaClO}_4$ . High-purity  $\text{N}_2$  was used to remove carbon dioxide and molecular oxygen from samples and to provide an inert gas atmosphere during all measurements. A combined electrode (E-331, Aurora Sci. Co., Shanghai, China) connected to a PHS-3TC pH meter was used to measure pH. Standard solutions of NaOH, HCl,  $\text{HL}^1$  and  $\text{VOSO}_4$  were employed to perform the potentiometric titrations.  $\text{VOSO}_4/\text{HL}^1$  system as a representative of these complexes was studied by pH-potentiometric titrations because the three N-substituted biguanido–oxovanadium complexes synthesized have similar coordination geometries. The protonation constants of the ligand  $\text{HL}^1$  were determined by titrating in 40 mL of ligand solution ( $3.0 \times 10^{-3}$  M) acidified by HCl (2 times ligand). The stability constants of the oxovanadium(IV)

complexes were determined by titrating in 40 mL of solution containing the ligand ( $3.0 \times 10^{-3}$  M) acidified by HCl and  $\text{VOSO}_4$  ( $1.5 \times 10^{-3}$  M) with standardized NaOH (0.09598 M) solution using a microsyringe. For  $\text{HL}^1$ , more than 180 data points in the pH range of 2.74–11.93, and for  $\text{VO}/\text{HL}^1$ , more than 220 data points in the pH range of 4.17–11.80 were used for subsequent analysis.

## Expression and purification of human PTPs

PTP1B, TCPTP, SHP-1 were expressed in *E. coli* as described previously (Yuan et al. 2009). HePTP, constructed as the pGEX-4T-GST-ΔHePTP expression vector containing human HePTP catalytic domain was also expressed and purified (Yuan et al. 2009) with minor modifications. The only difference was that the supernatant was directly loaded onto a Glutathione-Sepharose 4B column and eluted with washing buffer 1 (25 mM Tris, 2 mM 2-ME, 0.15 M NaCl, 2 mM EDTA, 0.1 % Triton X-100, pH 8.0), washing buffer 2 (25 mM Tris, 2 mM 2-ME, 0.15 M NaCl, 2 mM EDTA, pH 8.0) and elution buffer (50 mM Tris, 10 mM glutathione, pH 8.0), respectively.

## Protein tyrosine phosphatase inhibition assays

Protein tyrosine phosphatase activities were measured as similarly as described previously using *p*-nitrophenol phosphate (*p*-NPP) as the substrate (Montalibet et al. 2005; Yuan et al. 2009). The assays were performed in 20 mM MOPS buffer, pH 7.2, containing 50 mM NaCl and 2 mM GSH. The complexes were dissolved in DMSO ( $10^{-2}$  M), and diluted to various concentrations, then further diluted 10 times into enzyme-MOPS buffer solutions for activity studies. Inhibition assays were performed in the same buffer on a 96-well plate in 100  $\mu\text{L}$  volumes. The PTPs were

**Table 1** Synthesis and analysis of three biguanido–oxovanadium complexes

Compounds	Yield (% on V)	Element analysis(%), calcd/found			IR( $\text{cm}^{-1}$ ) $\nu_{\text{C}=\text{N}}^{\text{a}}$ , $\nu_{\text{V}=\text{O}}^{\text{b}}$	UV–Vis in DMF $\lambda_{\text{max}}/\text{nm}(\epsilon, \text{M}^{-1} \text{cm}^{-1})$
		C	H	N		
1	0.62 g (39)	28.16/28.92	6.50/6.37	41.04/42.16	1635 s, 938 s	375 (120), 560 (43)
2	0.51 g (20)	46.96/46.38	6.31/5.60	27.38/28.38	1630 s, 949 s	554 (14)
3	0.66 g (31)	34.62/34.64	6.05/6.01	33.64/33.25	1640 s, 933 s	561(20)

<sup>a</sup> Free ligand, 1,640 ( $\text{HL}^1 \cdot \text{HCl}$ ), 1,643 ( $\text{HL}^2 \cdot \text{HCl}$ ), 1,645  $\text{cm}^{-1}$  ( $\text{HL}^3 \cdot \text{HCl}$ )

<sup>b</sup> 995  $\text{cm}^{-1}$  in  $\text{VOSO}_4$

diluted to the final concentrations of 60, 250, 320 and 200 nM for PTP1B, TCPTP, HePTP and SHP-1 respectively. Ten microlitre of complex with various concentrations was mixed to 83  $\mu\text{L}$  of enzyme solution for 30 min. Then 2  $\mu\text{L}$  of *p*-NPP (0.1 M) substrate was added. After incubation for 30 min at room temperature, the assays were terminated by the addition of 5  $\mu\text{L}$  of 2 M NaOH. The  $A_{405}$  was measured on a microplate reader.  $\text{IC}_{50}$  values were obtained by fitting the concentration-dependent inhibition curves by use of the program Origin. All data points were carried out in triplicates. Solutions of the oxovanadium complexes were all freshly prepared before each experiment. The inhibition kinetic analysis was performed according to Eq. (1) (Ember et al. 2008).

$$v = \frac{V_{\max}[S]}{K_m \left(1 + \frac{[I]}{K_i}\right) + [S]} \quad (1)$$

where  $V_{\max}$  is the maximum initial velocity,  $K_m$  for the corresponding constant for substrate,  $S$  for the substrate,  $I$  for the inhibitor,  $K_i$  for the inhibition constant at varied substrate concentrations, derived from the slope of the Lineweaver–Burk plots. Inhibition constants were determined by measuring initial hydrolysis rates at different substrate and inhibitor concentrations.

#### Fluorescence spectroscopic studies on the interactions between complex 1 and PTP1B

Fluorescence spectra with 280 nm excitation were recorded with a Perkin Elmer LS-50B fluorescence spectrophotometer. The bandwidths used for the excitation and the emission were 5 nm. For titration experiments, the concentration of PTP1B was  $2 \times 10^{-7}$  M (2 mL), and aliquots of complex 1 (4  $\mu\text{L}$ ) were added and the solution was left to equilibrate for 5 min in MOPS buffer (20 mM MOPS, 500 mM NaCl, 2 mM GSH, pH 7.2) at room temperature.

## Results and discussion

### Infrared spectra of the complexes

As shown in Table 1, compared with that of  $\text{VO}_2\text{SO}_4$  ( $995\text{ cm}^{-1}$ ), the  $\text{V}=\text{O}$  stretching frequencies for all complexes 1–3 shift to lower frequencies at 938, 949 and  $933\text{ cm}^{-1}$ , respectively. The  $\text{C}=\text{N}$  stretching

frequencies in the biguanido–oxovanadium(IV) complexes shift to lower frequencies ( $1635$ ,  $1630$  and  $1640\text{ cm}^{-1}$ ) compared to those in the free ligands ( $1,640$  in  $\text{HL}^1\cdot\text{HCl}$ ,  $1,643$  in  $\text{HL}^2\cdot\text{HCl}$  and  $1,645\text{ cm}^{-1}$  in  $\text{HL}^3$ ) as well. The IR data suggest the formation of biguanido–oxovanadium(IV) complexes with  $\text{V}-\text{N}$  coordination in the complexes. The elemental analysis data of the three biguanido–oxovanadium complexes indicate that the molar ratios of the ligand to  $\text{VO}(\text{II})$  are 2:1, consisting with the formula of  $[\text{VO}(\text{L}^1)_2]\cdot\text{H}_2\text{O}$  (1),  $[\text{VO}(\text{L}^2)_2]\cdot 2\text{H}_2\text{O}$  (2) and  $[\text{VO}(\text{L}^3)_2]\cdot\text{H}_2\text{O}$  (3), respectively.

### Solution chemistry

#### UV–Vis spectra

Electronic absorption spectra (Fig. 1) of the complexes were measured in DMF solution due to their poor water solubility. Based on the species of these complexes containing  $\text{V}=\text{O}$  group with a  $\text{VO}(\text{N}_2\text{N}_2)$  coordination mode, the electronic spectra of the complexes in DMF solutions are analyzed in  $\text{C}_{4v}$  symmetry. There are four energy levels of d-orbitals in this perturbation and the order of these orbitals is in turn  $x^2 - y^2$  ( $b_1$ )  $>$   $z^2$  ( $a_1$ )  $>$   $xy$  ( $b_2$ )  $>$   $xz$ ,  $yz$  ( $e$ ). In other words, three d–d transitions (bands I, II and III) may be observed with different intensities, although not all are necessarily allowed. In fact, ligands  $\text{HL}^{1-3}$  are all bidentate chelated ligands, making symmetry lower than  $\text{C}_{4v}$ . Complex 1 shows two d–d bands at 560 (II,  ${}^2\text{B}_2 \rightarrow {}^2\text{B}_1$ ) and 375 nm (III,  ${}^2\text{B}_2 \rightarrow {}^2\text{A}_1$ ), but

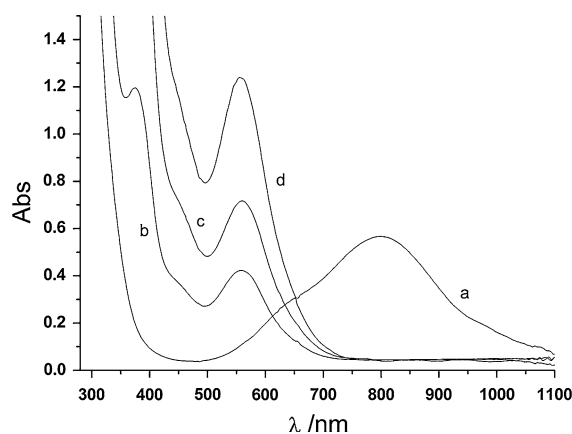


**Fig. 1** Electronic absorption spectra of complexes 1–3 in DMF **a**  $[\text{VO}_2\text{SO}_4] = 1.0 \times 10^{-2}$  M; **b**  $[1] = 1.0 \times 10^{-2}$  M; **c**  $[2] = 1.0 \times 10^{-1}$  M; **d**  $[3] = 1.0 \times 10^{-1}$  M

complex **2** displays only one d–d band at 554 nm (II). Meanwhile, complex **3** reveals a d–d band at 561 (I,  $^2B_2 \rightarrow ^2E$ ) (Lever 1984).

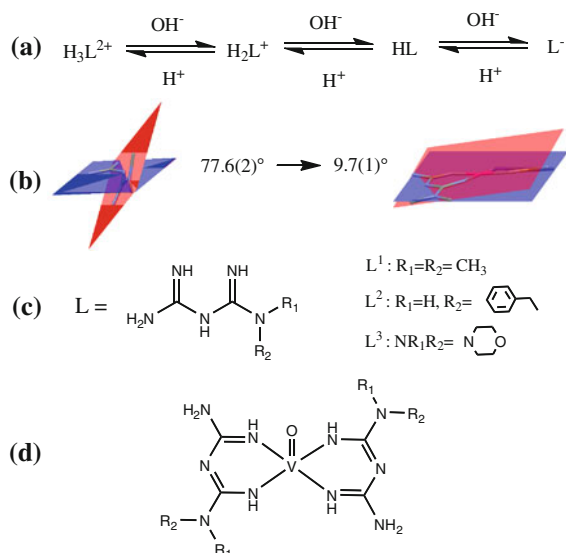
The species of biguanide derivatives are pH dependent in aqueous solution. The X-ray structures of biguanides clearly show that the ligands have the forms of diprotonation ( $H_3L^{2+}$ ), monoprotonation ( $H_2L^+$ ), neutral (HL) and deprotonation ( $L^-$ ) (Bishop et al. 2001, 2002, 2006; Igashira-Kamiyama et al. 2006; Lu et al. 2004a, b, c; Lu and Zhu 2003; Marchi et al. 1999; Moucharafieh et al. 1978; Su et al. 2005; Zheng et al. 2007; Zhu et al. 2002a, b, c, 2003a, b)(Scheme 1).

### Equilibrium constant calculations

The protonation and stability constants were calculated from the pH-titration data. The species formed in the systems were characterized by general equilibrium processes defined by Eq. (2) (omitted charges for simplicity) with the program SUPERQUAD program (Gans et al. 1996) to calculate the corresponding constants.

$$p(VO) + qL^1 + rH = (VO)_p L_q^1 H_r, \quad (2)$$

$$\beta_{pqr} = \frac{[(VO)_p L_q^1 H_r]}{[VO]^p [L]^q [H]^r}$$



**Scheme 1** **a** Species of biguanide compounds in acid–base solutions; **b** the change of dihedral angle between planes of guanide groups in free ligand and chelate complexes; **c** structural diagrams of ligands; **d** proposed structures of complexes **1–3**

The conventions notation has been used: negative indices for H in the formulas indicate either the dissociation of groups which do not deprotonate in the absence of VO(II) coordination, or hydroxo ligands. During the calculations, the values of  $pK_w$  is  $-13.78$  and the constants of hydrolysis species of VO(II) are taken into account (Table 2).

### Speciation in aqueous solution

In order to obtain more information about solution property of the complexes, the species of  $VO/L^1$  system in aqueous solution was studied from equilibrium constants of potentiometric titration. The protonation constants of the ligand and the formation constants of some species in the mixed aqueous solution of  $VOSO_4$  and ligands ( $VO:L = 1:2$ ) are given in Table 2. As a comparison,  $pK_a$  values of the ligand at 302 K and constants of some hydrolysis species of  $VO^{2+}$  are also listed in Table 2. Based on these data, the species distribution diagrams as a function of pH and titration curves are shown in Fig. 2.

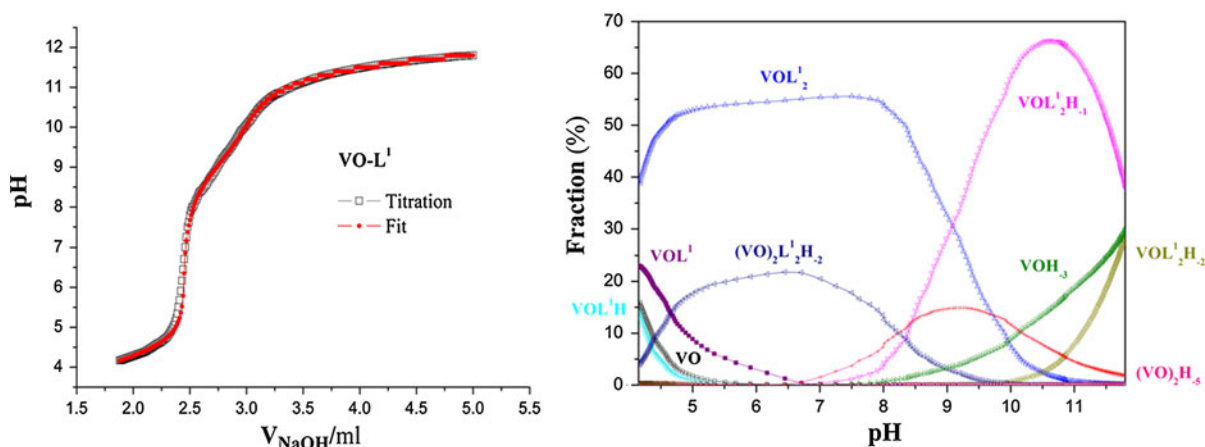
The distribution curves suggest that the predominant species in the range of pH 7–7.5 are  $[VOL_2^1]$  and  $[(VO)_2L_2^1H_{-2}]$ . When pH increases, both  $[VOL_2^1]$  and  $[(VO)_2L_2^1H_{-2}]$  species are transformed to  $[VOL_2^1H_{-1}]$  and some hydrolysis species of  $VO^{2+}$ . At physiological pH, the percentage of mononuclear  $[VOL_2^1]$  species is about 55 % while dinuclear  $[(VO)_2L_2^1H_{-2}]$  is about 20 %. Both species are over 90 % based on the total amount of vanadium.

### Binding of complex **1** with PTP1B: fluorescence spectroscopic evidence

The interactions between complex **1** and PTP1B were investigated by fluorescence spectroscopy in 20 mM MOPS buffer, pH 7.2. The effect of **1** on the fluorescence spectra of PTP1B is shown in Fig. 3. It is apparent that the fluorescence intensity of PTP1B at 335 nm (mainly from Trp residues) decreases gradually with the addition of **1**, suggesting binding between **1** and the enzyme. PTP1B contains six Trp residues, including one in the WPD loop close to the active site. The fluorescence quenching may arise from the binding of the biguanido–oxovanadium species on the enzyme, probably at the active site.

$p([\text{VO}(\text{II})])$	$q(\text{L}^1)$	$r(\text{H}^+)$	Species	$\text{p}K_{\text{a}1}, \text{p}K_{\text{a}2}, \log \beta$	Note
0	1	1	LH	11.69(1), 11.5	This work or ref <sup>b</sup>
0	1	2	$\text{LH}_2^+$	2.70(2), 2.8	This work or ref <sup>b</sup>
2	0	-1	$[(\text{VO})_2\text{H}_{-1}]^{3+}$	-5.94	Ref <sup>c</sup>
2	0	-2	$[(\text{VO})_2\text{H}_{-2}]^{2+}$	-6.95	Ref <sup>c</sup>
1	0	-3	$[(\text{VO})\text{H}_{-3}]^-$	-18.0	Ref <sup>c</sup>
2	0	-5	$[(\text{VO})_2\text{H}_{-5}]^-$	-22	Ref <sup>c</sup>
1	1	0	$[(\text{VO})\text{L}]^+$	10.66(4)	This work
1	2	0	$[(\text{VO})\text{L}_2]$	21.39(6)	This work
1	1	1	$[(\text{VO})\text{LH}]^{2+}$	14.60(7)	This work
1	2	-1	$[(\text{VO})\text{L}_2\text{H}_{-1}]^-$	12.31(5)	This work
1	2	-2	$[(\text{VO})\text{L}_2\text{H}_{-2}]^{2-}$	0.38(6)	This work
2	2	-2	$[(\text{VO})_2\text{L}_2\text{H}_{-2}]$	15.72(5)	This work

<sup>c</sup> Buglyó et al. (2000)





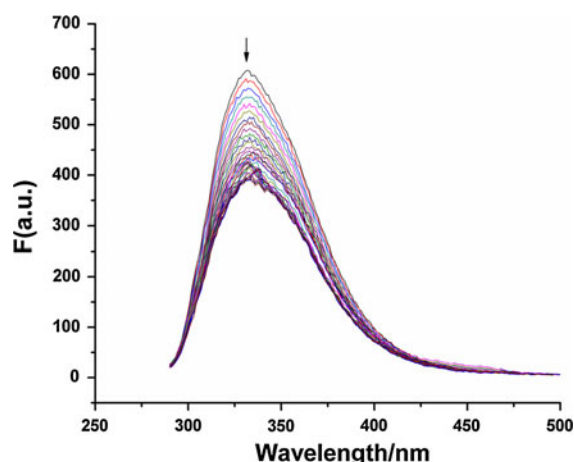


**Fig. 3** Fluorescence emission spectra of the titration of PTP1B ( $2.0 \times 10^{-7}$  M) with **1** ( $0.4\text{--}8.0 \times 10^{-7}$  M) in MOPS buffer (20 mM MOPS, 500 mM NaCl, 2 mM GSH, pH 7.2)

vanadium complexes. The comparison of the inhibitory effects of the three complexes indicates that complex **3** is about twofold less potent against PTP1B, TCPTP and HePTP than complexes **1**, and **2**, while complex **2** inhibits SHP-1 more strongly (about three to fourfold) than the other two complexes. This inhibition profile suggests that the structures of the ligands may have some effects on different PTPs. Morpholine ring appears to influence the binding of complex **3** to PTP1B, TCPTP and HePTP, but phenyl may be helpful for the binding of complex **2** to SHP-1. Compared with ternary vanadium complexes of tridentate Schiff bases and polypyridyl derivatives (Gao et al. 2009; Lu et al. 2010, 2011; Yuan et al. 2009, 2010), these biguanido–oxovanadium complexes display less potent against PTP1B. Therefore, the structures of ligands on vanadium complexes possibly influence the potency and selectivity against PTPs.

#### Inhibition mode of the biguanido–oxovanadium complexes on PTP1B and ALP

In order to evaluate the inhibition mode of biguanido–oxovanadium complexes on PTP1B and

ALP, inhibiting kinetics were measured at varying substrate concentrations in the absence or presence of inhibitors with different concentrations. The rates of enzyme-catalyzed reactions were determined and analyzed using Lineweaver–Burk plots. The Lineweaver–Burk plots give a family of lines intercepting on the  $1/v$  axis, exhibiting typical competitive inhibition which suggests binding of the oxovanadium species at the active sites on the enzymes (Figs. 5, 6, 7, LB plot data not shown for ALP tested with complexes **1** and **2**).

The  $K_i$  values for complexes **1** and **2** against PTP1B are estimated to be 42 and 45 nM, respectively, while the  $K_i$  for complex **3** is 58 nM (Figs. 5, 6, 7). The  $K_i$  values for ALP are determined to be 37 and 15  $\mu$ M for complexes **1** and **2**, respectively.

#### Biological relevance

pH-potentiometric titrations in aqueous solutions indicate that complex **1** exists as both mononuclear  $[\text{VOL}_2^1]$  and dinuclear  $[(\text{VO})_2\text{L}_2\text{H}_{-2}]$  species at physiological pH. Although the population of the mononuclear species is obviously much more than that of the dinuclear species, based on the current data, we can not tell if one or both of the species can inhibit the PTPs, or which one is more efficient. However, our results demonstrate clearly that the biguanido–oxovanadium complexes can bind PTPs and inhibit them efficiently with certain degree of selectivity. The detailed relationship between the structures of vanadium complexes and their inhibitory effects against PTPs need further investigation using other available systems.

Animal investigations with STZ-diabetic rats reveal that bi-functional biguanido–oxovanadium complex  $\text{VO}(\text{L}^1)_2$  was comparable to BMOV in lowering blood glucose levels (Woo et al. 1999). In the present study, we investigated the inhibitory effects of the biguanido–oxovanadium complexes against four PTPs and alkaline phosphatase. The results indicate that these biguanido–oxovanadium complexes are potent inhibitors against four PTPs, but obviously less potent

**Table 3**  $\text{IC}_{50}$  (nM) of complexes on PTPs and ALP

Complexes	PTP-1B	TCPTP	HePTP	SHP-1	ALP
<b>1</b>	86	109	218	2,380	33,000
<b>2</b>	105	129	191	813	17,000
<b>3</b>	157	152	413	2,800	17,000

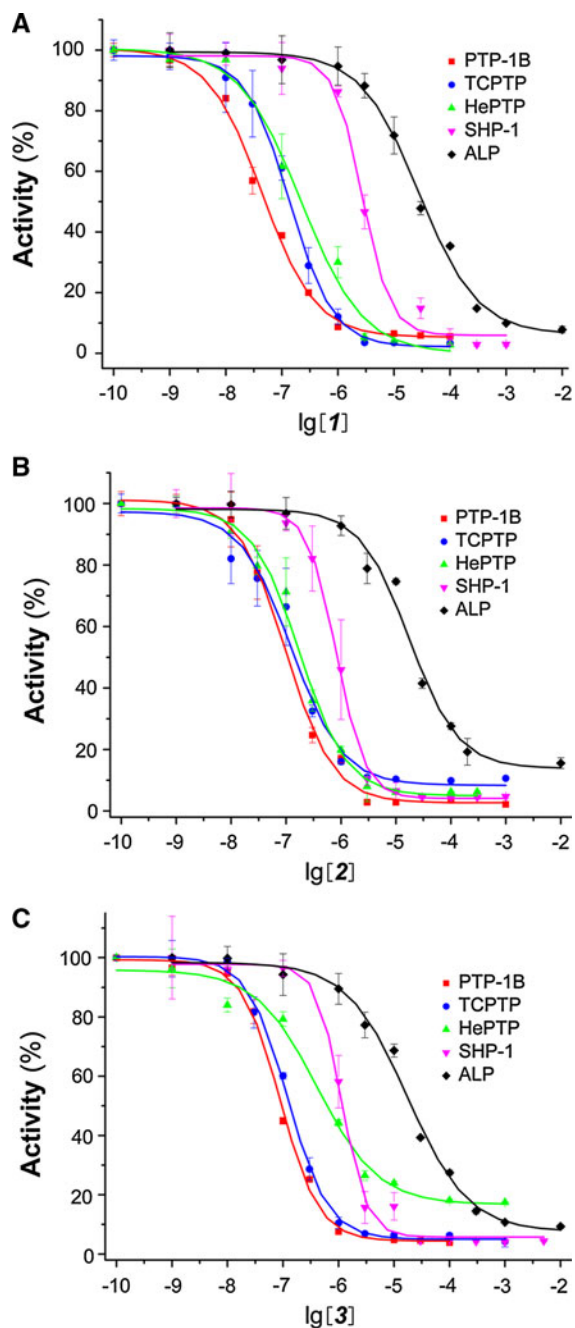


**Fig. 4** Dose-dependent inhibition of complexes (a **1**, b **2**, and c) on PTPs and ALP

against ALP, similar to those observed for BMOV in inhibiting PTP1B and ALP (Li et al. 2008). The complexes inhibit both PTP1B and ALP with a competitive inhibition model. Our results also reveal that the vanadium complexes do not inhibit the PTPs with the same potency, but display certain degree of

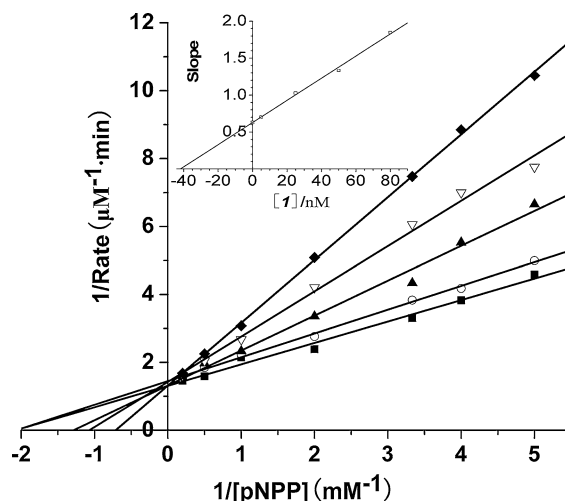


**Fig. 5** Lineweaver–Burk plots of  $1/v$  ( $\text{min } \mu\text{M}^{-1}$ ) versus  $1/[p\text{NPP}]$  ( $\text{mM}^{-1}$ ) at five fixed concentrations of complex **1** on the PTP1B, filled square 0.0, circle 5.0, filled triangle 25, white down-pointing triangle 50, filled diamond 80 ( $\text{nM}^{-1}$ ); inset the slope versus the concentration of complex **1** to determine the inhibition constant

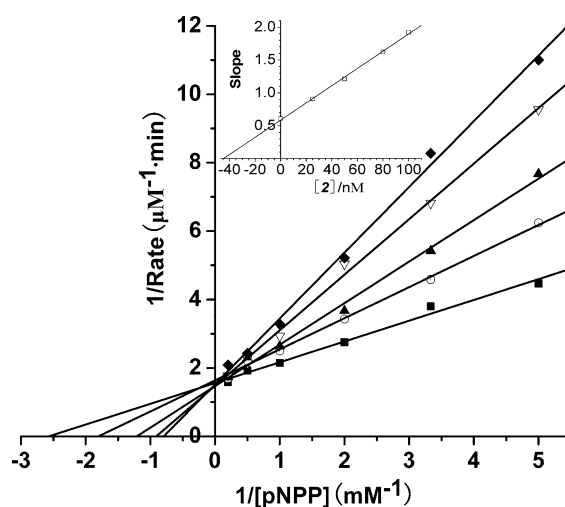


**Fig. 6** Lineweaver–Burk plots of  $1/v$  ( $\text{min } \mu\text{M}^{-1}$ ) versus  $1/[p\text{NPP}]$  ( $\text{mM}^{-1}$ ) at five fixed concentrations of complex **2** on the PTP1B, filled square 0.0, circle 25, filled triangle 50, white down-pointing triangle 80, filled diamond 100 ( $\text{nM}^{-1}$ ); inset the slope versus the concentration of complex **2** to determine the inhibition constant

selectivity. Peters' study (Peters et al. 2003) also shows that BMOV can inhibit human PTP1B, human cytoplasmic low molecular weight phosphotyrosyl protein phosphatase (HCPTPA), and src homology 2 phosphatase 2 (SHP2) with almost the same potency, but about tenfold more potent against human protein



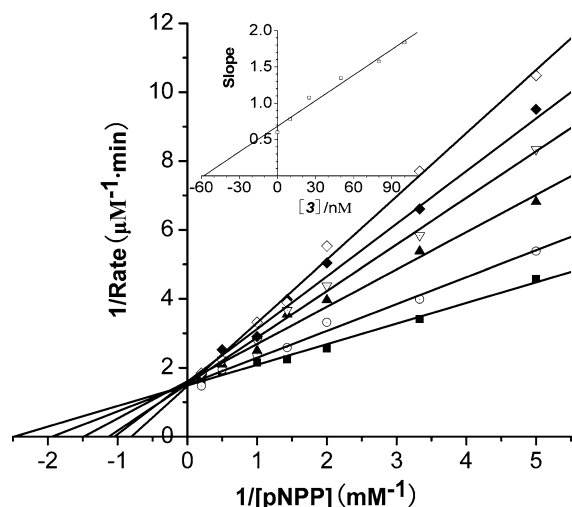


**Fig. 7** Lineweaver–Burk plots of  $1/v$  ( $\text{min } \mu\text{M}^{-1}$ ) versus  $1/[p\text{NPP}]$  ( $\text{mM}^{-1}$ ) at six fixed concentrations of complex **3** on the PTP1B, filled square 0.0, circle 10, filled triangle 25, white down-pointing triangle 50, filled diamond 80, diamond 100 ( $\text{nM}^{-1}$ ); inset the slope versus the concentration of complex **3** to determine the inhibition constant

tyrosine phosphatase b (HPTPb). Our previous study shows that  $[\text{VO(IV)}(\text{SAA})(\text{bpy})]$  complexes selectively inhibit PTP1B over the other two phosphatases SHP-1 (Src homology phosphatase 1) and TCPTP (T-cell protein tyrosine phosphatase), nevertheless oxovanadium glutamate complex inhibits the PTP1B, TCPTP, SHP-1 and HePTP with almost same potency (Gao et al. 2009; Lu et al. 2010, 2011; Yuan et al. 2009, 2010). All these results indicate that although vanadium complexes generally lack specificity, ligands have some influence on the selectivity against different PTPs. The selectivity may be related to the structures of the vanadium complexes and PTPs. Among these four PTPs, PTP1B and TC-PTP are about 74 % identical in the catalytic domains. Thus it is anticipated that PTP1B inhibitors might also inhibit TC-PTP with equal potency (Iversen et al. 2002). However, HePTP is only about 30 % identical in its catalytic domain compared to PTP1B, but its structure displays classical PTP1B fold (Mustelin et al. 2005). This may be the reason why HePTP is just twofold to threefold less sensitive to the vanadium complexes. Although its three-dimensional structure closely resembles that of PTP1B, SHP-1 bears low sequence identity ( $\sim 38$  %) with the catalytic domain of PTP1B, and, there are several insertions and deletions on its surface loops (Yang et al. 1998). This may explain the

over tenfold less sensitivity to the vanadium complexes. In human beings, 81 PTPs have been identified with the ability to dephosphorylate phosphotyrosine (Alonso et al. 2004). As vanadium complexes generally lack selectivity towards PTPs, they may impose strong side effects when being used as anti-diabetes drugs. Nevertheless, ligands of vanadium complexes influence their inhibitory effects against different PTPs and thus may enable vanadium complexes displaying certain selectivity. Thus it is necessary to perform a wide investigation on the bioactivities of structurally different vanadium complexes on different PTPs. Such a study will be helpful for developing vanadium drugs with selectivity toward PTP1B and thus decreasing side effects.

In fact, not only vanadium complexes but also other metal complexes, such as Cu complexes, may be potential inhibitors against PTPs (Li et al. 2011; Lu and Zhu 2011; Ma et al. 2011a, b; Wang et al. 2010, 2011; Yuan et al. 2012). They may regulate cell process or produce toxic effects through PTP inhibition. Compared with small organic molecules, metal complexes have their own advantage. The coordination geometry and reactive feature such as catalytic properties, redox activities of metal ions make them possess more versatile structures and reactivities.

## Conclusions

In summary, our data indicate that the three biguanido-oxovanadium complexes can inhibit four human PTPs potentially with a typical competitive inhibition mode. The structures of the ligands have some influence on the potency and selectivity against different PTPs. These results suggest that by rational designing the structures of ligands, it may be possible to develop some vanadium compounds which have stronger selectivity against PTP1B.

**Acknowledgments** This work is financially supported by the National Natural Science Foundation of China (Grant Nos. 20471033, 21001070 and 21171109), the Research Fund for the Doctoral Program of Higher Education of China (20111401110002), the China Scholarship Council, the Province Natural Science Foundation of Shanxi Province of China (Grant Nos. 20051013, 2010011011–2, and 2011011009–1), the 100 Talents Program of Shanxi Province, University of Massachusetts Dartmouth Cranberry Research Program, and UMass Science & Technology Initiatives Fund, MA, USA.

## References

- Ala PJ, Gonneville L, Hillman M, Becker-Pasha M, Yue EW, Douty B, Wayland B, Polam P, Crawley ML, McLaughlin E, Sparks RB, Glass B, Takvorian A, Combs AP, Burn TC, Hollis GF, Wynn R (2006) Structural insights into the design of nonpeptidic isothiazolidinone-containing inhibitors of protein-tyrosine phosphatase 1B. *J Biol Chem* 281:38013–38021
- Alonso A, Sasin J, Bottini N, Friedberg I, Osterman A, Godzik A, Hunter T, Dixon J, Mustelin T (2004) Protein tyrosine phosphatases in the human genome. *Cell* 117:699–711
- Andersen JN, Jansen PG, Echwald SM, Mortensen OH, Fukada T, Del Vecchio R, Tonks NK, Møller NP (2004) A genomic perspective on protein tyrosine phosphatases: gene structure, pseudogenes, and genetic disease linkage. *FASEB J* 18:8–30
- Arena S, Benvenuti S, Bardelli A (2005) Genetic analysis of the kinase and phosphatome in cancer. *Cell Mol Life Sci* 62:2092–2099
- Bishop MM, Lindoy LF, Skelton BW, White A (2001) Proton controlled supramolecular assembly: a comparative structural study of bis(2-guanidinobenzimidazolo)nickel(II) with bis(2-guanidinobenzimidazole)nickel(II) nitrate and 2-guanidinobenzimidazole. *Su. Supramol Chem* 13:293–301
- Bishop MM, Lindoy LF, Skelton BW, White AH (2002) Modification of supramolecular motifs: some effects of incorporation of metal complexes into supramolecular arrays. *J Chem Soc, Dalton Trans*: 377–382
- Bishop MM, Coles SJ, Lindoy LF, Parkin A (2006) A systematic study of ligand intermolecular interactions in crystals of copper(II) complexes of bidentate guanidino derivatives. *Inorg Chim Acta* 359:3565–3580
- Buglyó P, Kiss E, Fábíán I, Kiss T, Sanna D, Garribba E, Micera G (2000) Speciation and NMR relaxation studies of VO(IV) complexes with several O-donor containing ligands: oxalate, malonate, maltolate and kojate. *Inorg Chim Acta* 306:174–183
- Byon JCH, Kusari AB, Kusari J (1998) Protein-tyrosine phosphatase-1B acts as a negative regulator of insulin signal transduction. *Mol Cell Biochem* 182:101–108
- Combs AP, Yue EW, Bower M, Ala PJ, Wayland B, Douty B, Takvorian A, Polam P, Wasserman Z, Zhu WY, Crawley ML, Pruitt J, Sparks R, Glass B, Modi D, McLaughlin E, Bostrom L, Li M, Galya L, Blom K, Hillman M, Gonneville L, Reid BG, Wei M, Becker-Pasha M, Klabe R, Huber R, Li YL, Hollis G, Burn TC, Wynn R, Liu P, Metcalf B (2005) Structure-based design and discovery of protein tyrosine phosphatase inhibitors incorporating novel isothiazolidinone heterocyclic phosphotyrosine mimetics. *J Med Chem* 48:6544–6548
- Crans DC, Smee JJ, Gaidamauskas E, Yang LQ (2004) The chemistry and biochemistry of vanadium and the biological activities exerted by vanadium compounds. *Chem Rev* 104:849–902
- Dewang PM, Hsu NM, Peng SZ, Li WR (2005) Protein tyrosine phosphatases and their inhibitors. *Curr Med Chem* 12:1–22
- Drake PG, Posner BI (1998) Insulin receptor-associated protein tyrosine phosphatase(s): role in insulin action. *Mol Cell Biochem* 182:79–89
- Elchebly M (1999) Increased insulin sensitivity and obesity resistance in mice lacking the protein tyrosine phosphatase-1B gene. *Science* 283:1544–1548
- Ember B, Kamenecka T, LoGrasso P (2008) Kinetic mechanism and inhibitor characterization for c-jun-N-terminal kinase 3 alpha 1. *Biochem* 47:3076–3084
- Gans P, Sabatini A, Vacca A (1996) Investigation of equilibria in solution. Determination of equilibrium constants with the HYPERQUAD suite of programs. *Talanta* 43:1739–1753
- Gao X, Lu L, Zhu M, Yuan C, Ma J, Fu X (2009) Inhibitory activities of some oxovanadium complexes with N-heterocyclic ligands against PTP1B/ALP. *Acta Chim Sinica* 67:929–936
- Huyer G, Liu S, Kelly J, Moffat J, Payette P, Kennedy B, Tsaprailis G, Gresser MJ, Ramachandran C (1997) Mechanism of inhibition of protein-tyrosine phosphatases by vanadate and pervanadate. *J Biol Chem* 272:843–851
- Igashira-Kamiyama A, Kajiwarra T, Konno T, Ito T (2006) Ferromagnetic coupling promoted by k(3)N: k(2)N bridging system. *Inorg Chem* 45:6460–6466
- Iversen LF, Andersen HS, Branner S, Mortensen SB, Peters GH, Norris K, Olsen OH, Jeppesen CB, Lundt BF, Ripka W, Møller KB, Møller NP (2000) Structure-based design of a low molecular weight, nonphosphorus, nonpeptide, and highly selective inhibitor of protein-tyrosine phosphatase 1B. *J Biol Chem* 275:10300–10307
- Iversen LF, Møller KB, Pedersen AK, Peters GH, Petersen AS, Andersen HS, Branner S, Mortensen SB, Møller NP (2002) Structure determination of T cell protein-tyrosine phosphatase. *J Biol Chem* 277:19982–19990
- Kenner KA, Anyanwu E, Olefsky JM, Kusari J (1996) Protein-tyrosine phosphatase 1B is a negative regulator of insulin- and insulin-like growth factor-I-stimulated signaling. *J Biol Chem* 271:19810–19816
- Klaman LD, Boss O, Peroni OD, Kim JK, Martino JL, Zabolotny JM, Moghal N, Lubkin M, Kim YB, Sharpe AH, Stricker-Krongrad A, Shulman GI, Neel BG, Kahn BB (2000) Increased energy expenditure, decreased adiposity, and tissue-specific insulin sensitivity in protein-tyrosine phosphatase 1B-deficient mice. *Mol Cell Biol* 20:5479–5489
- Lever ABP (1984) *Inorganic electronic spectroscopy*, 2nd edn. Elsevier, Amsterdam, p 385
- Li M, Ding W, Baruah B, Crans DC, Wang R (2008) Inhibition of protein tyrosine phosphatase 1B and alkaline phosphatase by bis(maltolato)oxovanadium (IV). *J Inorg Biochem* 102:1846–1853
- Li Y, Lu L, Zhu M, Wang Q, Yuan C, Xing S, Fu X, Mei Y (2011) Potent inhibition of protein tyrosine phosphatases by copper complexes with multi-benzimidazole derivatives. *Biometals* 24:993–1004
- Liljebriis C, Martinsson J, Tedenborg L, Williams M, Barker E, Duffy JES, Nygren A, James S (2002) Synthesis and biological activity of a novel class of pyridazine analogues as non-competitive reversible inhibitors of protein tyrosine phosphatase 1B (PTP1B). *Bioorg Med Chem* 10:3197–3212
- Lu LP, Zhu ML (2003) Bis{[N'-(E)-amino(imino)methyl]morpholinocarboximidamido}copper(II). *Acta Crystallogr Sect E* E59:m1086–m1088
- Lu L, Zhu M (2011) Metal-based inhibitors of protein tyrosine phosphatases. *Anti-Cancer Agents Med Chem* 11:164–171

- Lu LP, Yang P, Qin SD, Zhu ML (2004a) Bis[1,1-dimethylbiguanide(1-) $\kappa$ N<sup>2</sup>,N<sup>5</sup>]copper(II) monohydrate. *Acta Crystallogr Sect C* C60:m219–m220
- Lu LP, Zhang HM, Feng SS, Zhu ML (2004b) Two *N,N*-dimethylbiguanidium salts displaying double hydrogen bonds to the counter-ions. *Acta Crystallogr Sect C* C60:O740–O743
- Lu LP, Zhu ML, Yang P (2004c) Cocrystal of the [Mn<sup>IV</sup>(C<sub>2</sub>H<sub>7</sub>N<sub>5</sub>)<sub>3</sub>]<sup>4+</sup> ion and biguanidium: a double hydrogen-bond interaction with guanidinium-recognizing anions. *Acta Crystallogr Sect C* C60:M18–M20
- Lu L, Wang S, Zhu M, Liu Z, Guo M, Xing S, Fu X (2010) Inhibition protein tyrosine phosphatases by an oxovanadium glutamate complex, Na<sub>2</sub>[VO(Glu)<sub>2</sub>(CH<sub>3</sub>OH)] (Glu = glutamate). *Biometals* 23:1139–1147
- Lu L, Yue J, Yuan C, Zhu M, Han H, Liu Z, Guo M (2011) Ternary oxovanadium(IV) complexes with amino acid-Schiff base and polypyridyl derivatives: synthesis, characterization, and protein tyrosine phosphatase 1B inhibition. *J Inorg Biochem* 105:1323–1328
- Ma L, Lu L, Zhu M, Wang Q, Gao F, Yuan C, Wu Y, Xing S, Fu X, Mei Y, Gao X (2011a) Dinuclear copper complexes of organic claw: potent inhibition of protein tyrosine phosphatases. *J Inorg Biochem* 105:1138–1147
- Ma L, Lu L, Zhu M, Wang Q, Li Y, Xing S, Fu X, Gao Z, Dong Y (2011b) Mononuclear copper(II) complexes with 3,5-substituted-4-salicylidene-amino-3,5-dimethyl-1,2,4-triazole: synthesis, structure and potent inhibition of protein tyrosine phosphatases. *Dalton Trans* 40:6532–6540
- Maccari R, Paoli P, Ottana R, Jacomelli M, Ciurleo R, Manao G, Steindl T, Langer T, Vigorita MG, Camici G (2007) 5-Arylidene-2,4-thiazolidinediones as inhibitors of protein tyrosine phosphatases. *Bioorg Med Chem* 15:5137–5149
- Marchi A, Marvelli L, Cattabriga M, Rossi R, Neves M, Bertolasi V, Ferretti V (1999) Technetium(V) and rhenium(V) complexes of biguanide derivatives. Crystal structures. *J Chem Soc Dalton Trans* 12:1937–1944
- Montalibet J, Skorey KI, Kennedy BP (2005) Protein tyrosine phosphatase: enzymatic assays. *Methods* 35:2–8
- Moucharafieh NC, Eller PG, Bertrand JA, Royer DJ (1978) Spectra and structure of tris-bidentate cobalt(III) complexes containing planar ligands. *Inorg Chem* 17:1220–1228
- Mustelin T, Tautz L, Page R (2005) Structure of the hematopoietic tyrosine phosphatase (HePTP) catalytic domain: structure of a KIM phosphatase with phosphate bound at the active site. *J Mol Biol* 354:150–163
- Na M, Cui L, Min BS, Bae K, Yoo JK, Kim BY, Oh WK, Ahn JS (2006) Protein tyrosine phosphatase 1B inhibitory activity of triterpenes isolated from *Astilbe Koreana*. *Bioorg Med Chem Lett* 16:3273–3276
- Nxumalo F, Glover NR, Tracey AS (1998) Kinetics and molecular modelling studies of the inhibition of protein tyrosine phosphatases by *N,N*-dimethylhydroxylamine complexes of vanadium(V). *J Biol Inorg Chem* 3: 534–542
- Peters KG, Davis MG, Howard BW, Pokross M, Rastogi V, Diven C, Greis KD, Eby-Wilkens E, Maier M, Evdokimov A, Soper S, Genbauffe F (2003) Mechanism of insulin sensitization by BMOV (bis maltolato oxo vanadium); unliganded vanadium (VO<sub>4</sub>) as the active component. *J Inorg Biochem* 96:321–330
- Posner BI, Faure R, Burgess JW, Bevan AP, Lachance D, Zhang-Sun G, Fantus IG, Ng JB, Hall DA, Lum BS (1994) Peroxovanadium compounds. A new class of potent phosphotyrosine phosphatase inhibitors which are insulin mimetics. *J Biol Chem* 269:4596–4604
- Ray P (1961) Complex compounds of biguanides and guanylureas with metallic elements. *Chem Rev* 61:313–359
- Rehder D (2003) Biological and medicinal aspects of vanadium. *Inorg Chem Commun* 6:604–617
- Reul BA, Amin SS, Buchet JP, Ongemba LN, Crans DC, Brichard SM (1999) Effects of vanadium complexes with organic ligands on glucose metabolism: a comparison study in diabetic rats. *Br J Pharmacol* 126:467–477
- Saltiel AR, Kahn CR (2001) Insulin signalling and the regulation of glucose and lipid metabolism. *Nature* 414:799–806
- Shechter Y (2003) Historic perspective and recent developments on the insulin-like actions of vanadium; toward developing vanadium-based drugs for diabetes. *Coord Chem Rev* 237:3–11
- Shrestha S, Bhattarai BR, Lee K-H, Cho H (2007) Mono- and disalicylic acid derivatives: PTP1B inhibitors as potential anti-obesity drugs. *Bioorg Med Chem* 15:6535–6548
- Sparks RB, Polam P, Zhu W, Crawley ML, Takvorian A, McLaughlin E, Wei M, Ala PJ, Gonville L, Taylor N, Li Y, Wynn R, Burn TC, Liu PCC, Combs AP (2007) Benzothiazole benzimidazole (S)-isothiazolidinone derivatives as protein tyrosine phosphatase-1B inhibitors. *Bioorg Med Chem Lett* 17:736–740
- Su YL, Lu LP, Li XM, Zhu ML (2005) Bis(biguanido- $\kappa$ N,N')copper(II) dihydrate. *Acta Crystallogr Sect E* E61:m910–m912
- Thompson KH, Lichter J, LeBel C, Scaife MC, McNeill JH, Orvig C (2009) Vanadium treatment of type 2 diabetes: a view to the future. *J Inorg Biochem* 103:554–558
- Wang Q, Lu L, Yuan C, Pei K, Liu Z, Guo M, Zhu M (2010) Potent inhibition of protein tyrosine phosphatase 1B by copper complexes: implications for copper toxicity in biological systems. *Chem Commun* 46:3547–3549
- Wang Q, Zhu M, Lu L, Yuan C, Xing S, Fu X (2011) Potent inhibition of protein tyrosine phosphatases by quinquedentate binuclear copper complexes: synthesis, characterization and biological activities. *Dalton Trans* 40:12926–12934
- Willsky GR, Goldfine AB, Kostyniak PJ, McNeill JH, Yang LQ, Khan HR, Crans DC (2001) Effect of vanadium(IV) compounds in the treatment of diabetes: in vivo and in vitro studies with vanadyl sulfate and bis(maltolato)oxovanadium(IV). *J Inorg Biochem* 85:33–42
- Winter CL, Lange JS, Davis MG, Gerwe GS, Downs TR, Peters KG, Kasibhatla B (2005) A nonspecific phosphotyrosine phosphatase inhibitor, bis(maltolato)oxovanadium(IV), improves glucose tolerance and prevents diabetes in Zucker diabetic fatty rats. *Exp Biol Med* 230:207–216
- Woo LC, Yuen VG, Thompson KH, McNeill JH, Orvig C (1999) Vanadyl-biguanide complexes as potential synergistic insulin mimics. *J Inorg Biochem* 76:251–257
- Xie J, Seto CT (2007) A two stage click-based library of protein tyrosine phosphatase inhibitors. *Bioorg Med Chem* 15: 458–473
- Yang J, Liang X, Niu T, Meng W, Zhao Z, Zhou GW (1998) Crystal structure of the catalytic domain of protein-tyrosine phosphatase SHP-1. *J Biol Chem* 273:28199–28207

- Yuan C, Lu L, Gao X, Wu Y, Guo M, Li Y, Fu X, Zhu M (2009) Ternary oxovanadium(IV) complexes of ONO-donor Schiff base and polypyridyl derivatives as protein tyrosine phosphatase inhibitors: synthesis, characterization, and biological activities. *J Biol Inorg Chem* 14:841–851
- Yuan C, Lu L, Wu Y, Liu Z, Guo M, Xing S, Fu X, Zhu M (2010) Synthesis, characterization, and protein tyrosine phosphatases inhibition activities of oxovanadium(IV) complexes with Schiff base and polypyridyl derivatives. *J Inorg Biochem* 104:978–986
- Yuan C, Zhu M, Wang Q, Lu L, Xing S, Fu X, Jiang Z, Zhang S, Li Z, Li Z, Zhu R, Ma L, Xu L (2012) Potent and selective inhibition of T-cell protein tyrosine phosphatase (TCPTP) by a dinuclear copper(ii) complex. *Chem Commun* 48: 1153–1155
- Zhang ZY (2001) Protein tyrosine phosphatases: prospects for therapeutics. *Curr Opin Chem Biol* 5:416–423
- Zhang S, Zhang ZY (2007) PTP1B as a drug target: recent developments in PTP1B inhibitor discovery. *Drug Discov Today* 12:373–381
- Zheng LL, Zhang WX, Oin LJ, Leng JD, Lu JX, Tong ML (2007) Isolation of a pentadentate ligand and stepwise synthesis, structures, and magnetic properties of a new family of homo- and heterotrimeric complexes. *Inorg Chem* 46:9548–9557
- Zhu ML, Lu LP, Jin XL, Yang P (2002a) Trichloro(1,1-dimethylbiguanidium- $\kappa N^3$ )zinc(II). *Acta Crystallogr Sect C* C58:m158–m159
- Zhu ML, Lu LP, Yang P, Jin XL (2002b) Bis(1,1-dimethylbiguanido)copper(II) octahydrate. *Acta Crystallogr Sect E* E58:m217–m219
- Zhu ML, Lu LP, Yang P, Jin XL (2002c) Bis(1,1-dimethylbiguanido)nickel(II). *Acta Crystallogr Sect E* E58:m272–m274
- Zhu ML, Lu LP, Yang P (2003a) *N,N*-Dimethylbiguanidium nitrate. *Acta Crystallogr Sect E* E59:o586–o588
- Zhu ML, Yang P, Liu LP (2003b) *N*-Phenethylbiguanidium tetrachlorozincate(II). *Acta Crystallogr Sect E* E59:m91–m94
- Zinker BA, Rondinone CM, Trevillyan JM, Gum RJ, Clampit JE, Waring JF, Xie N, Wilcox D, Jacobson P, Frost L, Kroeger PE, Reilly RM, Koterski S, Opgenorth TJ, Ulrich RG, Crosby S, Butler M, Murray SF, McKay RA, Bhanot S, Monia BP, Jirousek MR (2002) PTP1B antisense oligonucleotide lowers PTP1B protein, normalizes blood glucose, and improves insulin sensitivity in diabetic mice. *Proc Natl Acad Sci USA* 99:11357–11362